PCCP

Accepted Manuscript

ROYAL SOCIETY OF CHEMISTRY

www.rsc.org/pccp

PCCP

RSCPublishing

PAPER

Pulsed Electron-Electron Double Resonance Spectroscopy between a High-Spin Mn^{2+} Ion and a Nitroxide Spin Label

Cite this: DOI: 10.1039/xoxxoooooox

Received ooth January 2012,
Accepted ooth January 2012

DOI: 10.1039/xoxxoooooox

www.rsc.org/

D. Akhmetzyanov,[a] J. Plackmeyer,[a] B. Endeward,[a] V. Denysenkov[a] and T. F. Prisner[a]

Pulsed Electron-Electron Double Resonance (PELDOR) has attracted considerable attention for biomolecular applications, as it affords precise measurements of distances between pairs of spin labels in the range of 1.5-8 nm. Usually nitroxide moieties incorporated by site-directed spin labelling with cysteine residues are used as spin probes in protein systems. Recently, naturally occurring cofactors and metal ions have also been explored as paramagnetic spin species for such measurements. In this work we investigate the performance of PELDOR between a nitroxide spin label and a high-spin Mn^{2+} ion in a synthetic model compound at Q-band (34 GHz) and G-band (180 GHz). We demonstrate that the distances obtained with high-frequency PELDOR are in good agreement with structural predictions. At Q-band frequencies experiments have been performed by probing either the high-spin Mn^{2+} ion or the nitroxide spin label. At G-band frequencies we have been able to detect changes in the dipolar oscillation frequency, depending on the pump-probe positions across the g-tensor resolved nitroxide EPR spectrum. These changes result from the restricted mobility of the nitroxide spin label in the model compound. Our results demonstrate that the high-spin Mn^{2+} ion can be used for precise distance measurements and open the doors for many biological applications, as naturally occurring Mg^{2+} sites can be readily exchanged for Mn^{2+}.

Introduction

Determination of distances in the nanometer range is an important issue for structural characterisation of macromolecules. Pulsed Electron-Electron Double Resonance (PELDOR)[1] has become a valuable method for such applications in material science and structural biology[2,3] allowing the determination of distances in the 1.5-8 nm range from measurement of the magnetic dipole-dipole coupling between two paramagnetic sites. So far, nitroxide spin labels specifically attached to proteins[4] or nucleic acids[5] have been used as paramagnetic probes in biological systems. Only a few examples have been reported, where naturally occurring paramagnetic cofactors, for example, amino acid radicals,[6] metal ions[7] or iron-sulfur clusters[8,9] were used for PELDOR measurements. Recently, chelate complexes with Gd^{3+} [10,11] or Mn^{2+} ions[12] have been used as paramagnetic tags attached to proteins. Due to the high electronic spin multiplicity of these metal ions, it is beneficial to perform EPR experiments at higher magnetic field strengths.[13]

The Mn^{2+} ion is especially attractive for biological applications, since several enzymes[14] and membrane proteins naturally contain this paramagnetic marker. Moreover, due to the very similar ionic radius and identical electric charge of Mn^{2+} and Mg^{2+} ions, Mn^{2+} can easily replace Mg^{2+}, an essential cofactor for many enzymes, nucleic acid molecules and nucleotide binding domains.[15] Thus, PELDOR in combination with Electron-Nuclear Double Resonance (ENDOR) spectroscopy, is an ideal tool for structural characterisation of such intrinsic metal sites in biomolecules, which in many cases undergo long range structural rearrangements and changes in the ligand sphere within the catalytic function.[16,17]

The high-spin Mn^{2+} ion has an electronic spin of $S = 5/2$. In addition the 100% naturally abundant ^{55}Mn isotope has a

[a] Goethe University Frankfurt am Main, Institute of Physical and Theoretical Chemistry and Center for Biomolecular Magnetic Resonance, Max von Laue Str. 7, 60438 Frankfurt am Main, Germany. E-mail: prisner@chemie.uni-frankfurt.de

† Electronic Supplementary Information (ESI) available: EPR spectrum of compound **6**. Phase memory time measurements on compound **4** at Q-band and G-band frequencies and on compound **6** at Q-band frequencies. PELDOR time traces without background subtraction of compound **4** at Q-band, experimental parameters, background functions, experimental and fitted Pake patterns. Q-band EPR experiments upon pumping and detecting on Mn^{2+} ion spin system on compound **4** and on compound **6**. Simulated PELDOR time traces at G-band frequencies on compound **4** without background function, parameters of simulations. MS spectrum of compound **4**. See DOI: 10.1039/b000000x/

nuclear spin of $I = 5/2$. Such high-spin multiplicities lead to rather complex EPR spectra in disordered systems at low magnetic fields.[18] However, at higher magnetic field, when the electron Zeeman splitting is considerably larger than the Zero-Field Splitting (ZFS), the six allowed hyperfine lines of the central electron spin transition ($|m_S = -1/2, m_I\rangle \rightarrow |m_S = 1/2, m_I\rangle$) become narrow and indicative. The line narrowing of the central transition can be assessed by second-order perturbation theory. This reveals that the linewidth scales inversely with the external magnetic field as D^2/B_0, assuming a ZFS asymmetry parameter of $E = 0$.[18] Moreover, the intensities of the forbidden hyperfine transitions ($\Delta m_S = \pm1$ $\Delta m_I = \pm1$ and $\Delta m_S = \pm1$ $\Delta m_I = \pm2$) become significantly reduced.[18] Thus, the EPR spectrum of a disordered Mn^{2+} system simplifies considerably at higher magnetic field.

The EPR signals resulting from the different electron spin sublevels ($|m_S,m_I\rangle \rightarrow |m_S\pm1,m_I\rangle$) of the Mn^{2+} ion all have different transition moments. Therefore, the Rabi oscillation frequency of the central electron spin transition of an Mn^{2+} ion spin system is 3 times higher compared to a nitroxide electron spin ($S = 1/2$) at high magnetic fields. These differences in transition moments can be used to separate the different electron spin transitions by their Rabi nutation frequencies.[19] However, this phenomenon further complicates pulsed EPR experiments, especially at low magnetic fields, as spectrally overlapping allowed and forbidden transitions are all excited simultaneously by the microwave pulses, although to a different extent.

Here we performed PELDOR measurements at two magnetic field strengths (1.2 T and 6.4 T corresponding to electron excitation frequencies of 33.7 GHz (Q-band) and 180 GHz (G-band), respectively) on a nitroxide-Mn^{2+} model compound in order to investigate in detail the performance of this experiment while pumping either on the nitroxide spin system or Mn^{2+} ion spin system.

Results and discussion

Synthesis

The synthesis of the model compound **4** with a distance of approximately 2.7 nm between the unpaired electron of the nitroxide and the Mn^{2+} ion[20-22] is schematically represented in Fig. 1. Sonogashira coupling of **1** with 4'-(4-ethynylphenyl)-2,2':6',2''-terpyridine **2** yielded the nitroxide substituted terpyridine ligand **3**. The heteroleptic Mn^{2+}-terpyridine complex **4** was obtained as the hexafluorophosphate by mixing equimolar amounts of **3** with [Mn(terpyridine)Cl_2] and precipitation under excess of NH_4PF_6.

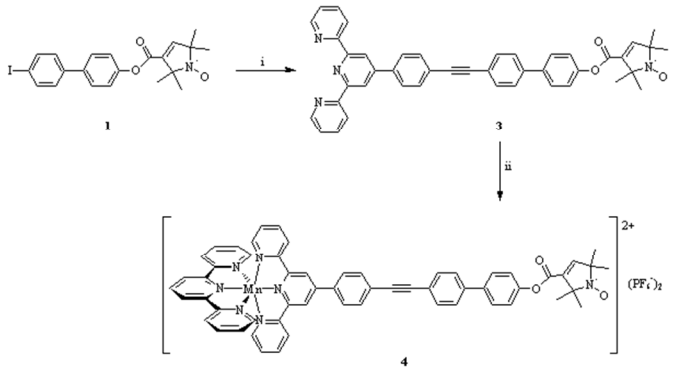

Fig. 1. Scheme of the synthesis of the ligand **3** and the model compound **4**. Reagents and conditions: (i) 4'-(4-ethynylphenyl)-2,2':6',2''-terpyridine **2**, $Pd(PhCN)_2Cl_2$, CuI, TBAB, $P(Ph)_3$, Et_2NH/THF, room temperature, 16 h. (ii) (a) [Mn(terpyridine)Cl_2], MeOH/CH_2Cl_2, 45 – 50 °C, 1.5 h; (b) NH_4PF_6, MeOH.

EPR spectroscopy

The PELDOR experiments on the heteroleptic Mn^{2+}-terpyridine complex **4** were performed at Q-band (33.7 GHz) and G-band (180 GHz) frequencies. The field-swept echo-detected EPR spectra at both frequencies are shown in Fig. 2. At Q-band frequencies (Fig. 2 left) a broad and featureless EPR signal from the Mn^{2+} ion spin system can be observed with the comparably narrow nitroxide EPR signal superimposed. Despite the fact that pulse lengths (32 ns) and repetition time (0.8 ms) were optimised for the much faster relaxing Mn^{2+} ion spins in this experiment, the nitroxide signal still shows a larger relative intensity. The sample temperature was set to 5 K in order to achieve longer transversal relaxation (T_2) time for Mn^{2+} ion spins, as the latter limits the length of the observable time window. The Mn^{2+} ions hyperfine lines of the central electron spin transition $|-1/2, m_I\rangle \rightarrow |1/2, m_I\rangle$ are not resolved at Q-band frequencies which indicates the presence of relatively large ZFS parameters for this molecule. In another study of Mn^{2+} bis(terpyridine) complexes it was found that the ZFS parameter D is strongly dependent on the structure of the terpyridine moiety and on the solvent.[23,24] ZFS parameters for the Mn^{2+} bis(terpyridine) complex in acetonitrile were given as: $D = -1.54$ GHz and $E = 0.3$ GHz.[23] Attaching a nitroxide linker to one of the terpyridine moieties, as is the case with the heteroleptic Mn^{2+}-terpyridine complex **4** and using 2-Methyltetrahydrofuran as solvent may lead to different ZFS parameters. An EPR spectrum of compound **6** (scheme is presented in Fig. S1) a derivative of compound **4** without the nitroxide moiety is shown in Fig. S2.

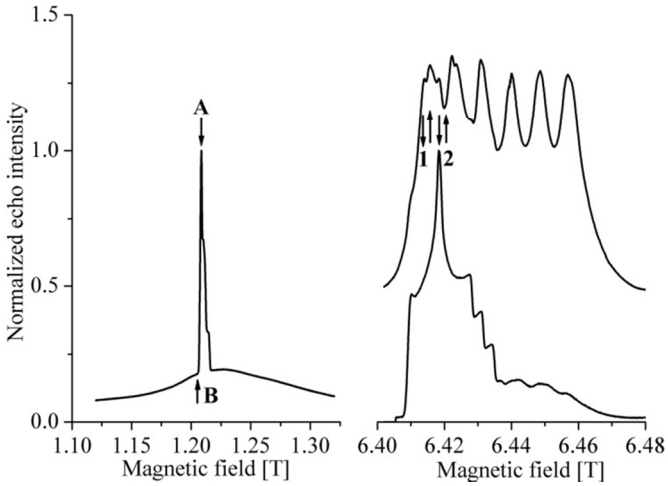

Fig. 2. Field-swept echo-detected EPR spectrum of the heteroleptic Mn^{2+}-terpyridine complex **4**.
Left - Spectrum recorded at Q-band frequencies and a temperature of 5 K; arrows at the field positions A and B illustrating the probe and pump positions for the PELDOR experiments. Pulse lengths and repetition time of the pulse sequence are optimised for the Mn^{2+} ion spin system at field position B.
Right - Spectra recorded at G-band frequencies and a temperature of 10 K. Upper spectrum: pulse lengths and repetition time of the pulse sequence are optimised for the Mn^{2+} ion spin system at one of the central hyperfine lines. Lower spectrum: pulse lengths and repetition time of the pulse sequence are optimised for the nitroxide spin system at the position of maximum absorption in the nitroxide spectrum. The

sets of arrows at field positions 1 and 2 illustrate the pump and probe excitation positions used for the PELDOR experiments. Within each set (1 or 2) the arrows up and down represent the probe and pump positions respectively.

Field-swept echo-detected EPR spectra of the heteroleptic Mn^{2+}-terpyridine complex **4** at G-band frequencies are shown in Fig. 2 on the right side. As described previously, the linewidth of the central electron spin transitions narrow at higher fields. Therefore, the sextet of hyperfine lines for this transition can clearly be resolved at G-band frequencies (Fig. 2 upper right spectrum). Since the overall Mn^{2+} ion spectral shape is very smooth and reveals no characteristic features related to the ZFS, a broad statistical distribution of the ZFS parameters of the Mn^{2+} ion of the compound **4** must exist. A similar broad statistical distribution of the ZFS parameters was also observed for the Gd^{3+} complexes in frozen solution.[25] The overlapping EPR spectra corresponding to the Mn^{2+} ion and nitroxide spins can be distinguished by changing the length of the pulses and the experimental repetition time because of the different transition moments and longitudinal relaxation times (T_1) of the two species. Such a procedure has already been demonstrated for the Gd^{3+}-nitroxide spin system at X- and Q-band frequencies.[26]

PELDOR experimental time traces of the heteroleptic Mn^{2+}-terpyridine complex **4** at Q-band frequencies are presented in Fig. 3 together with respective fits. In both cases, when probing either on the Mn^{2+} ion or nitroxide spin systems, pronounced dipolar oscillations are visible, reflecting the rigid structure of compound **4**.

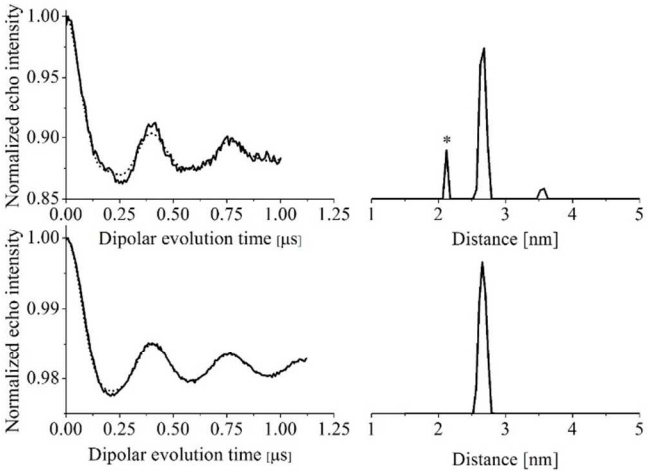

Fig. 3. Background-corrected PELDOR time traces obtained at Q-band frequencies. The solid lines are experimental time traces, the dotted lines are the fits by Tikhonov regularisation.[29] The upper row shows the PELDOR time traces and distance distribution functions obtained by pumping on position A (nitroxide, as depicted in Fig. 2) and probing on position B (Mn^{2+}). The lower row shows the traces for pumping on position B (Mn^{2+}) and probing on position A (nitroxide). The pump-probe frequency difference is 90 MHz in both cases. Both experiments are performed at 5 K. The peak at 2.1 nm marked by the asterisk is described in the text.

For PELDOR experiments at Q-band frequencies a 90 MHz offset between pump and probe frequencies was used. This separation is the upper limit that could be achieved with the experimental setup. This value was chosen such that when probing the Mn^{2+} ion spins and pumping on the maximum of the nitroxide spectrum, a negligible amount of nitroxide spins are excited by the detection pulses. Excitation of the nitroxide spins by the detection pulses would reduce the modulation depth. Moreover, we assume that level mixing of the dipolar coupled Mn^{2+}-nitroxide spin system, due to the pseudo-secular terms of the dipolar coupling Hamiltonian, could be significantly minimised by choosing a pump-probe frequency offset that considerably exceeds the dipolar coupling constant. In general, the contribution from the pseudo-secular terms is larger for a dipolar coupled pair of high-spin centres compared to a pair of spin-1/2 centres, as demonstrated for a Gd^{3+}-Gd^{3+} system.[27] However, if only one centre in the pair has a high spin quantum number, the contribution from the pseudo-secular terms is reduced, as proposed for a Gd^{3+}-nitroxide pair compared to a Gd^{3+}-Gd^{3+} system.[28] It is assumed, that this situation will also apply for the Mn^{2+}-nitroxide system studied here.

Orientation selection effects at Q-band frequencies are expected to be negligible. When pumping and probing at the maximum of the nitroxide EPR spectrum the orientation selectivity is poor at this frequency. In the case of pumping and probing Mn^{2+} the orientation selectivity is also assumed to be small due to a broad statistical distribution of the ZFS parameters. Therefore, a Tikhonov regularisation with the complete Pake pattern as the integral kernel function[29] can be used to determine the distance between two spins within the molecule. DeerAnalysis[29] has been used to obtain the distance distribution functions in both cases.

The PELDOR time trace obtained by probing the nitroxide and pumping on the Mn^{2+} spins (Fig. 3 lower row), revealed a narrow distance distribution with a single distance of 2.65 nm and a full width at half maximum of only 0.15 nm (The Fourier-transformed Pake pattern is shown in Fig. S3). When pumping on the nitroxide and probing the Mn^{2+} spins (Fig. 3 upper row), the same distance of 2.65 nm was extracted from the dipolar evolution function. A Tikhonov regularisation, performed with DeerAnalysis 2013 with a regularisation parameter of 0.01, was used in both cases. Validation using different fitting conditions for the background function provided an error of about 0.05 nm. Hence, the extracted distance is in good agreement with the predicted interspin distance of 2.7 nm.

The distance distribution pattern obtained from the PELDOR time trace by probing the Mn^{2+} spins contains a ghost peak at a 2.1 nm (asterisk in Fig. 3). A possible explanation of this is the occurrence of nuclear modulation effects in the PELDOR trace (a two-pulse ESEEM experiment is depicted in Fig. S2 of the supporting information). Due to the short transversal relaxation time of Mn^{2+} spins, tau-averaging was not used in the PELDOR experiment, as it would reduce the signal/noise ratio. Control experiments were performed where pump and probe pulses were applied only on the Mn^{2+} of compound **4** or compound **6**. A detailed explanation of these experiments is given in section 4 of the supporting information. These experiments revealed oscillations which are likely to also be present in the PELDOR time trace obtained by probing the Mn^{2+} spins. Another possible explanation may be insufficient fulfillment of the high-field approximation at Q-band frequencies, so that ZFS induced contributions to the secular term of the dipolar coupling Hamiltonian,[28] occur in the PELDOR time trace when probing the Mn^{2+} spins. Such effects are not included in the standard analysis of PELDOR time traces.

The appearance of additional satellite peaks in the distance distribution pattern has also been observed at X- and Q-band PELDOR experiments of a Gd^{3+}-nitroxide spin system.[26] The features were attributed to a violation of the high-field

approximation and, for a part of the molecular ensemble, to effects arising from excitation of transitions other than the $|-1/2\rangle \leftrightarrow |1/2\rangle$.[26] In the case of the Mn^{2+}-nitroxide system studied here it is assumed that the central electron spin transition, including forbidden ^{55}Mn hyperfine transitions, is excited to a much larger extent than the other electron transitions. A detailed study of the distortions in PELDOR induced by ZFS and ZFS distribution when the high-field approximation is violated has been performed on Gd^{3+} species.[28] It was shown, that the ratio $3D/g\mu B_0$ defines the magnitude of distortions appearing in PELDOR for the Gd^{3+}-nitroxide spin system. Larger ZFS parameters induce a higher degree of level mixing and thus deviations from the normal undistorted case. This is particularly dramatic when the external magnetic field is not aligned along the canonical orientations of the ZFS frame. Nevertheless, for the cases where the ratio $3D/g\mu B_0$ is 2/3 (corresponding to a D value of 2 GHz at X-band frequencies) it was shown that the dipolar frequency pattern reveals only modest deviation from the expected pattern. These distortions appear as an artificial broadening of the distance distribution without significant shifts of the mean distance. For the D values $\leq$ 600 MHz at X-band frequencies the distortions are negligibly small. For the data obtained at Q-band frequencies distortions of the distance distribution were expected to be negligible, and a conventional analysis of the PELDOR time traces can be safely applied for values of D < 2 GHz.[28] The values given above are specific for Gd^{3+} however analogous results are expected for high-spin Mn^{2+}.[28]

The Q-band data presented here indicate that for the Mn^{2+}-nitroxide complex only weak distortions in the PELDOR trace are induced by ZFS. This does not lead to a shift of the mean distance within the experimental error, nor to broadening of the distance distribution. However, a detailed study of the high-field approximation violation in high-spin Mn^{2+} systems has yet to be performed in more detail.

As expected, the modulation depth λ is much lower when pumping on Mn^{2+}. In this case a modulation depth of only 2% was achieved under our experimental conditions. A detailed calculation of the excitation efficiency is complicated because of spectral overlap and the fact that spectral shape, population and nutation frequencies differ for all the individual electron spin transitions. In addition, the hyperfine coupling of the Mn^{2+} electronic spin system with the ^{55}Mn nuclear spin system and ZFS causes level mixing ($|m_S,m_I\rangle$ and $|m_S,m_I\pm1\rangle$; $|m_S,m_I\rangle$ and $|m_S,m_I\pm2\rangle$)[18] further complicating the picture especially at Q-band frequencies. Nevertheless, a rough approximation can be done by comparing the pump pulse excitation width with the overall spectral width. A pump pulse length of 20 ns corresponds to an excitation bandwidth of about 40 MHz and the overall Mn^{2+} linewidth is $8D+5A$ (from first order perturbation theory). Assuming a ZFS parameter D of about 1.5 GHz and hyperfine coupling of about 250 MHz, this corresponds to a Mn^{2+} spectral width of 13.25 GHz. This rough analysis predicts a value of λ = 1%. Although, this approximation is rather imprecise, it roughly corresponds to the experimentally observed value of 2%.

In the other case, when pumping on the nitroxide spin system, a modulation depth of 11% was experimentally achieved. At Q-band frequencies the nitroxide spectral width is about 280 MHz, leading to a pump efficiency of about 30% when pumping on the maximum of the spectrum. B_1 inhomogeneity of the Q-band resonator leads to a value of 25% for the modulation depth. This has been experimentally observed for nitroxide biradicals with our experimental setup. Therefore, the experimental λ value observed on the heteroleptic Mn^{2+}-terpyridine complex **4** is roughly a factor of 2 less than expected.

To investigate orientation selection effects for a high-spin Mn^{2+} ion coupled with a nitroxide spin, we performed PELDOR experiments at G-band frequencies, where the anisotropy of the nitroxide g-tensor is fully resolved (as shown in Fig. 2 lower right spectrum). Two PELDOR experimental time traces for different pump positions on the nitroxide spectrum and probing the Mn^{2+} (Fig. 2) spins are depicted in Fig. 4 together with corresponding simulations based on the geometry of the molecule.

The experimentally observed modulation depths at both pump positions at G-band are a factor of 2.8 smaller compared to the predictions (analysis is described below). The fact that the observed modulation depths upon pumping on the nitroxide are smaller compared to the predictions both at Q- and G-band frequencies, indicates that the sample might also contain Mn^{2+} complexes that are not covalently coupled to the nitroxide moiety. This is supported by the appearance of a peak with m/z corresponding to Mn^{2+} bis(terpyridine) complex in the ESI mass spectrum (Fig. S7). A reduced modulation depth was also observed for a Gd^{3+}-Gd^{3+} spin system.[27] It has been hypothesised that for this spin system the effect is caused by the influence of pseudo-secular terms of the dipolar coupling Hamiltonian that contribute to the PELDOR signal. However, in the case of the Mn^{2+}-nitroxide system studied here this effect is assumed to be negligible.

In the G-band data the modulation depth and frequency differ between the two PELDOR time traces taken at positions 1 and 2. This indicates orientation selection in the time traces when pumping on the nitroxide. Therefore, the analysis of the PELDOR time traces cannot be done by Tikhonov regularisation with the complete Pake pattern as the integral kernel function. Thus, simulations of the two PELDOR time traces at G-band frequencies were performed using the known orientation of the nitroxide moiety compared to the direction of the linker[22] and the excited orientations of the nitroxide with respect to $\boldsymbol{B}_0$ (calculated with EasySpin[30] software, shown as insets in Fig. 4) upon pumping at position 1 or 2 (Fig. 4). The simulations used a fixed interspin distance of 2.7 nm (dotted lines in Fig. 4) and a Gaussian distance distribution width of 0.15 nm. The modulation depths of the simulations were corrected to those achieved experimentally to allow better visualisation (dash-dotted lines in Fig. 4).

For the simulation of the orientationally selective G-band experiments the geometry between the nitroxide moiety and the dipolar axis was taken from the structure predictions (Fig. 1). Flexibility of the linker and the rotation of the nitroxide moiety around the linker axis of the complex was not explicitly included but only modeled by a Gaussian distance distribution, adjusted to fit the experimentally observed damping of the dipolar oscillations. Nevertheless the dipolar oscillation frequencies observed experimentally upon pumping on different positions in the nitroxide spectrum as well as the relative modulation depths are reproduced nicely by the simulations (the simulated time traces without background are depicted in Fig. S8).

It is important to note, that the orientation selection analysis, which takes only the secular term of the dipolar coupling Hamiltonian into account, reproduced very well the experimentally observed dipolar oscillation frequencies and the ratio of the modulation depths at different selected spectral positions of the pumped nitroxide spin system.

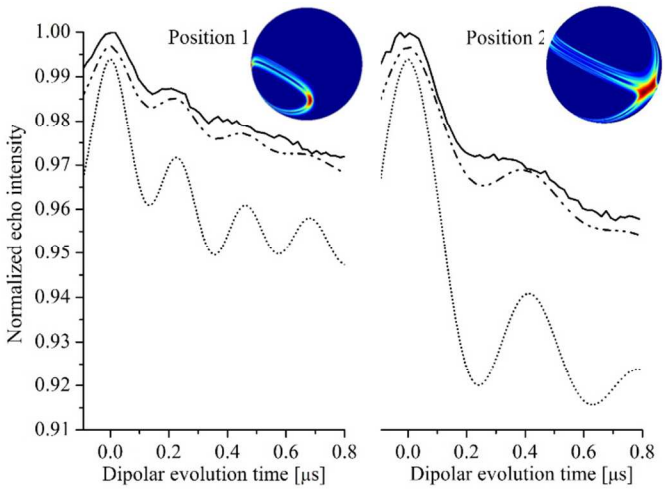

Fig. 4. PELDOR time traces at G-band without background subtraction. The solid lines represent experimental data; the dotted lines represent the simulation with calculated modulation depths and with the fixed interspin distance of 2.7 nm; the dash-dotted lines is the simulation where Gaussian distance distribution was included and experimental modulation depths were adapted to the experimental values. The pump-probe frequency offset is set to 60 MHz. The intermolecular background function used for the simulations is adjusted to fit the experimental data. Insets to the figure show the excited orientations of the nitroxide spin system in the g-tensor frame.

Experimental

Synthesis of the heteroleptic Mn^{2+}-terpyridine complex 4

General. All reactions were performed with exclusion of air under argon, employing standard Schlenk techniques. Reagent-grade solvents and chemicals were used without further purification, except where stated otherwise. Dry solvents were purchased (Aldrich, ACROS) and thoroughly degassed prior to use. Diethylamine (ACROS) was freshly distilled from CaH_2. Solvents and reagents for Sonogashira cross-couplings were degassed by freeze-pump-thaw cycles. 4'-(4-Bromophenyl)-2,2':6',2''-terpyridine **5**[31], $[Mn(terpy)Cl_2]$[32] were synthesised according to the literature cited. 4'-(4-Ethynylphenyl)-2,2':6',2''-terpyridine **2** was obtained from 4-ethynylbenzaldehyde[33] by the method of Winter and coworkers.[34] Synthesis of 1-oxyl-2,2,5,5-tetramethyl-pyrrolin-3-carboxylic acid 4'-iodobiphenyl-4yl-ester **1** as well as the equipment for analytic observations were already described elsewhere.[35]

(1-Oxyl-2,2,5,5-tetramethyl-pyrrolin-3-carboxylic acid-(4'-(4-[2,2':6',2'']terpyridin-4'-yl-phenylethynyl)-biphenyl-4-yl)-ester) 3. Bis(benzonitrile)dichloropalladium(II) (43 mg, 0.11 mmol) and 1-oxyl-2,2,5,5-tetramethyl-pyrrolin-3-carboxylic acid 4'-iodobiphenyl-4yl-ester (367 mg, 0.75 mmol) were suspended in 150 mL diethylamine. Addition of 15 mL THF resulted in a yellow solution. To the stirred mixture CuI (26 mg, 0.13 mmol) and tetrabutylammoniumbromide (50 mg, 0.15 mmol) were added, followed by a solution of 4'-(4-ethynylphenyl)-2,2':6',2''-terpyridine (250 mg, 0.75 mmol) and triphenylphosphine (28 mg, 0.11 mmol) in 50 mL diethylamine and 10 mL THF. The resulting orange solution was stirred for 16 h at room temperature. All solvents were removed *in vacuo* and the remaining orange solid was treated with NH_4Cl solution (1 M, 150 mL) and dichloromethane (150 mL). The organic phase was washed with water and brine, dried (Na_2SO_4) and stripped from the solvent. The residue was recrystallised from methanol. A pale yellow solid was finally obtained by filtration. Yield: 313 mg (0.46 mmol, 62%). Anal. Calcd for **3** ($C_{44}H_{35}O_3N_4$ (667.78)): C, 79.14; H, 5.28; N, 8.39. Found: C, 78.68; H, 5.78; N, 7.76. ESI-MS: *m/z* 668.17 ($[M+H]^+$).

([4'-(4-Bromophenyl)-2,2':6',2''-terpyridine][2,2':6',2''-terpyridine]manganese(II)-bis-hexafluorophosphate) 6. 4'-(4-Bromophenyl)-2,2':6',2''-terpyridine **5** (39 mg, 0.10 mmol) and $[Mn(terpy)Cl_2]$ (36 mg, 0.10 mmol) were dissolved in 15 mL of methanol by stirring for 1 h. The resulting yellow mixture was heated to reflux for 4 h and filtered while still warm. To the filtrate 2 eq. of NH_4PF_6 (33 mg, 0.20 mmol) were added, which gave a pale yellow precipitate. After filtration the yellow solid was washed with methanol and diethyl ether and air dried. Yield: 52 mg (0.05 mmol, 50%). Anal. Calcd for **6** ($C_{36}H_{25}MnN_6P_2F_{12}Br$ (966.41)): C, 44.74; H, 2.61; N, 8.69. Found: C, 44.50; H, 2.56; N, 8.68.

([1-Oxyl-2,2,5,5-tetramethyl-pyrrolin-3-carboxylic acid-(4'-(4-[2,2':6',2'']terpyridin-4'-yl-phenylethynyl)-biphenyl-4-yl)-ester][2,2':6',2''-terpyridine]manganese(II)-bis-hexafluorophosphate) ($[Mn(terpy)(3)](PF_6)_2$) 4. $[Mn(terpy)Cl_2]$ (14.7 mg, 0.041 mmol) was dissolved in 8 mL of methanol by warming up the mixture slightly. The ligand **3** (27.1 mg, 0.041 mmol) dissolved in dichloromethane (3 mL) was added dropwise, resulting in an intensified yellow colour of the reaction mixture. The solution was warmed up to 45-50 °C for 30 min., after which a yellow solid precipitated. Stirring was continued at the same temperature for additional 60 min. After cooling to room temperature the solution was filtered. A solution of 4 eq. NH_4PF_6 (26.7 mg, 0.164 mmol) in methanol (1 mL) was added to the filtrate and a yellow precipitate was formed. For complete precipitation the mixture was stored over night at 4 °C. A yellow solid was obtained by filtration, washed with cold methanol and dried *in vacuo*. Yield: 27 mg (0.022 mmol, 53%). Anal. Calcd for **4** ($C_{59}H_{46}MnN_7O_3P_2F_{12}$ (1245.91)): C, 56.88; H, 3.72; N, 7.87. Found: C, 57.74; H, 3.89; N, 7.37. ESI-MS: *m/z* 477.1 ($[M-2PF_6]^{2+}$); 1100.7 ($[M-PF_6]^+$).

Pulsed EPR experiments

Pulsed EPR experiments were performed on a Bruker Elexsys E580 spectrometer using a ER5107D2 Q-band probehead and on a home built G-band EPR spectrometer.[36,37]

Q-band experiments were performed at a temperature of 5 K. The field-swept echo-detected EPR spectrum was recorded with pulses of 32 ns length, the power of the π/2 and π pulses, respectively, was adjusted for maximum echo intensity of the Mn^{2+} ion spin system at the detection position B (see Fig. 2); the pulse separation (here the time between front edges of the pulses) was 120 ns; the experimental repetition time was 0.8 ms. The four-pulse PELDOR sequence[38] was used for both Q- and G-band experiments. A Q-band PELDOR experiment in which the nitroxide spin system was pumped (at the maximum of the spectrum, position A in Fig. 2) was performed with pulse lengths of 20 ns (pump pulse) and 32 ns (detection pulses); the dipolar evolution time window was 1.6 μs. The power of the pump pulse was adjusted for maximum inversion efficiency of the nitroxide spins and the power of detection pulses were

adjusted for maximum echo intensity at position B. The experimental repetition time was 0.408 ms. Identical pulse lengths and pulse separations were used for the Q-band PELDOR experiment where the Mn^{2+} spin system was pumped (corresponding to the position B in Fig. 2 left). The power of the pump pulse was adjusted for maximum inversion efficiency of the Mn^{2+} spin system, whereas the power of the detection pulses were optimised for maximum echo intensity of the nitroxide signal. The experimental repetition time was 8.16 ms.

All G-band EPR experiments were performed at 10 K. The field-swept echo-detected EPR spectrum, optimised for Mn^{2+} spin system (the upper spectrum in Fig. 2, right) were recorded with pulse lengths of 22.5 and 32.5 ns for $\pi/2$ and π pulses, respectively. The length of the $\pi/2$ pulse is more than half the length of the π pulse due to relatively long (about 5 ns) rise and fall time for pulses on the G-band spectrometer. The microwave power was 30 mW for both pulses. The pulse separation (here the time between falling edge of the first pulse and front edge of the second pulse) was set to 300 ns and the repetition time to 1.1 ms. The adjustment of the pulse lengths was performed for maximum echo intensity at one of the ^{55}Mn hyperfine lines of the Mn^{2+} central transition. For the field-swept echo-detected EPR spectrum optimised for the nitroxide spin system, the pulse lengths were 40 and 75 ns for $\pi/2$ and π pulses, respectively. The pulse separation was set to 300 ns and the experimental repetition time to 77.5 ms. For PELDOR experiments the detection pulse lengths were 20 and 27.5 ns and the pump pulse length was 65 ns. The microwave power was 60 mW for all pulses. The dipolar evolution time window was 1.5 µs and the experimental repetition time was 1.1 ms.

Sample preparation for the EPR experiments

2-methyltetrahydrofuran (MTHF) was used as a solvent (Sigma-Aldrich). Dissolution of the compound **4** was achieved by counter ion exchange with the non-coordinating tetrakis [3,5-bis(trifluoromethyl)phenyl] borate (BAr^{F-}_4). Sodium tetrakis [3,5-bis(trifluoromethyl)phenyl] borate ($NaBAr^{F-}_4$), obtained from Alfa Aesar, was added to a mixture of the heteroleptic Mn^{2+}-terpyridine complex **4** and MTHF with 30 to 40-fold excess. After adding $NaBAr^{F-}_4$ the solution became yellow coloured and was fully dissolved after 15 to 20 minutes of vortex mixing. The concentration of the compound for the EPR measurements was approximately 200 µM. For EPR measurements the sample was transferred to 1 mm inner diameter quartz tubes (Q-band) and 0.4 mm inner diameter tubes (G-band).

Conclusions

PELDOR experiments on a molecule containing a high-spin Mn^{2+} ion and a nitroxide spin system were performed at Q- and G-band frequencies. Analysis of the PELDOR data recorded at Q-band reveals an interspin distance of 2.65 nm, which is in good agreement with the distance derived from the crystal structures of similar compounds. The PELDOR data recorded at G-band frequencies show a dependence of the dipolar oscillation frequency on the position of the pump pulse within the spectrum. Simulations taking the orientation selection of the nitroxide spin system into account are in good agreement with the experimentally observed orientationally selective PELDOR oscillation frequencies. Our results demonstrate that the high-spin Mn^{2+} ions can be used in conjunction with nitroxide spin labels for accurate distance determination. This provides interesting possibilities for applications to nucleotide binding domains of proteins and other biological systems. Extension of such studies to Mn^{2+}-Mn^{2+} spin pairs is under investigation in our laboratory.

Acknowledgements

The authors thank Dr. Philipp Spindler for assistance with first Q-band PELDOR measurements, Dr. Andriy Marko and Dr. Björn Corzilius for discussions and Dr. Alice Bowen for proofreading of the manuscript. The authors acknowledge financial support from the German Research Society DFG (GZ: PR 294/14-1).

References

1 A. Milov, A. Ponomarev and Yu. Tsvetkov, *Chem. Phys. Lett*., 1984, **110**, 67.
2 G. Jeschke, *Annu. Rev. Phys. Chem*., 2012, **63**, 419.
3 O. Schiemann and T. Prisner, *Q. Rev. Biophys*., 2007, **40**, 1.
4 W. Hubbell, A. Gross, R. Langen and M. Lietzow, *Curr. Opin. Struct. Biol.*, 1998, **8**, 649.
5 I. Krstic, B. Endeward, D. Margraf, A. Marko and T. Prisner, *Top. Curr. Chem*., 2012, **321**, 159.
6 V. Denysenkov, T. Prisner, J. Stubbe and M. Bennati, *Proc. Natl. Acad. Sci. U.S.A*., 2006, **103**, 13386.
7 I. van Amsterdam, M. Ubbink, G. Canters and M. Huber, *Angew. Chem. Int. Ed.*, 2003, **42**, 62.
8 C. Elsässer, M. Brecht and R. Bittl, *J. Am. Chem. Soc*., 2002, **124**, 12606.
9 M. Roessler, M. King, A. Robinson, F. Armstrong, J. Harmer and J. Hirst, *Proc. Natl. Acad. Sci. U.S.A.*, 2010, **107**, 1930.
10 A. Potapov, H. Yagi, T. Huber, S. Jergic, N. Dixon, G. Otting and D. Goldfarb, *J. Am. Chem. Soc*., 2010, **132**, 9040.
11 L. Garbuio, E. Bordignon, E. Brooks, W. Hubbell, G. Jeschke and M. Yulikov, *Phys. Chem. B*., 2013, **117**, 3145.
12 D. Banerjee, H. Yagi, T. Huber, G. Otting and D. Goldfarb, *J. Phys. Chem. Lett*., 2012, **3**, 157.
13 A. Raitsimring, C. Gunanathan, A. Potapov, I. Efremenko, J. Martin, D. Milstein and D. Goldfarb, *J. Am. Chem. Soc*., 2007, **129**, 14138.
14 I. Fridovich, *Ann. Rev. Biochem*., 1995, **64**, 97.
15 T. Schweins, K. Scheffzek, R. Aßheuer and A. Wittinghofer, *J. Mol. Biol.*, 1997, **266**, 847.
16 P. Manikandan, R. Carmieli, T. Shane, A. Kalb (Gilboa) and D. Goldfarb, *J. Am. Chem. Soc*., 2000, **122**, 3488.
17 M. Bennati, M. Hertel, J. Fritscher, T. Prisner, N. Weiden, M. Spörner, R. Hofweber, G. Horn and H. Kalbitzer, *Biochem*., 2006, **45**, 42.
18 G. Reed and G. Markham, *Biological Magnetic Resonance ed. by L. Berliner and J. Reuben*., 1984, **6**, 73.
19 A. Astashkin and A. Shweiger, *Chem. Phys. Lett*., 1990, **174**, 595.
20 A. Rompel, A. Bond and C. McKenzie, *Acta Cryst. E*., 2004, **E60**, m1759.
21 H.-G. Liu, Y.-C. Qiu and J.-Z. Wu, *Acta Cryst. E*., 2007, **E63**, m2393.
22 D. Margraf, D. Schuetz, T. Prisner and J. Bats, *Acta Cryst. E*., 2009, **E65**, o1784.
23 J. Gätjens, M. Sjödin, V. Pecoraro and S. Un, *J. Am. Chem. Soc*., 2007, **129**, 13825.

24 C. Duboc, M. Collomb, J. Pecaut, A. Deronzier and F. Neese, *Chem. Eur. J.*, 2008, **14**, 6498.
25 A. Raitsimring, A. Astashkin, O. Poluektov and P. Caravan, *Appl. Magn. Reson*., 2005, **28**, 281.
26 P. Lueders, G. Jeschke and M. Yulikov, *J. Phys. Chem. Lett.*, 2011, **2**, 604.
27 A. Potapov, Y. Song, T. Meade, D. Goldfarb, A. Astashkin and A. Raitsimring, *J. Magn. Reson.*, 2010, **205**, 38.
28 M. Yulikov, P. Lueders, M. Warsi, V. Chechik and G. Jeschke, *Phys. Chem. Chem. Phys.*, 2012, **14**, 10732.
29 G. Jeschke, V. Chechik, P. Ionita, A. Godt, H. Zimmermann, J. Banham, C. Timmel, D. Hilger and H. Jung, *Appl. Magn. Reson.*, 2006, **30**, 473.
30 S. Stoll and A. Schweiger, *J. Magn. Reson.*, 2006, **178**, 42.
31 W. Spahni and G. Calzaferri, *Helv. Chim. Acta*., 1984, **67**, 450.
32 C. Mantel, C. Baffert, I. Romero, A. Deronzier, J. Pecaut, M.-N. Collomb and C. Duboc, *Inorg. Chem.*, 2004, **43**, 6455.
33 W. Austin, N. Bilow, W. Kelleghan and K.S. Lau, *J. Org. Chem.*, 1981, **46**, 2280.
34 A. Winter, A.M. van den Berg, R. Hoogenboom, G. Kickelbick and U. Schubert, *Sythesis*., 2006, **17**, 2873.
35 B. Bode, J. Plackmeyer, T. Prisner and O. Schiemann, *J. Phys. Chem. A*, 2008, **112**, 5064.
36 M. Rohrer, O. Brügman, B. Kinzer and T. Prisner, *Appl. Magn. Res.*, 2001, **21**, 257.
37 V. Denysenkov, T. Prisner, J. Stubbe and M. Bennati, *Appl. Magn. Res.*, 2005, **29**, 375.
38 M. Pannier, S. Veit, A. Godt, G. Jeschke and H. Spiess, *J. Magn. Reson.*, 2000, **142**, 331.